Frontal Functional Connectivity Impairment in Early Stages of Alzheimer's Disease

Ivan Plaza-Rosales
University of Chile: Universidad de Chile https://orcid.org/0000-0002-2112-8439
Rodrigo Montefusco-Siegmund
Austral University: Universidad Austral
Samuel Madariaga
University of Chile: Universidad de Chile
Enzo Brunetti
Instituto de Neurocirugia e Investigaciones cerebrales Dr. Alfonso Asenjo
María Isabel Behrens
University of Chile: Universidad de Chile
Andrea Paula-Lima
University of Chile: Universidad de Chile
Pedro E. Maldonado (pedro@uchile.cl)
University of Chile: Universidad de Chile

Research Article

Keywords: early Alzheimer's Disease, EEG, Evoked potentials/Visual, Ocular movements, Coherence, Functional connectivity

Posted Date: September 21st, 2021

DOI: https://doi.org/10.21203/rs.3.rs-903120/v1

Abstract

Background

Many neurophysiological markers such as neuronal oscillations, cortical neuronal synchronization and long-range neuronal coupling have been suggested to permit the identification of early cognitive impairments in Alzheimer's disease (AD). However, it is still unclear whether alterations in long-range Functional Connectivity (FC) constitute part of early mechanisms in the initial stages of AD.

Methods

Eighteen participants (69-88 years old), classified as early AD and matching healthy controls, were evaluated while performing a virtual spatial navigation task. We combined electroencephalography (EEG) and eye movement recordings during the performance of a virtual version of the Morris Water Maze (VMWM), where participants had to find a submerged, invisible platform. The groups were compared in their navigation performance with different metrics of brain activity.

Results

We found that the subjects of both groups showed characteristic visual exploration patterns, with a central and over the horizontal midline exploration in controls and more peripheral and sparse fixations, in early AD subjects. In addition, regions in visual exploration between the groups were significantly different. The control group presented a marked occipital activity in the beta band (15-20 Hz) in comparison to the early AD group at early processing time. These differences in the beta band were much more robust in prefrontal regions with significant differences in the frontal cortex, which has been associated with spatial navigation tasks in addition to planning and decision making.

Conclusions

These results suggest that long-range Functional connectivity networks generated from early visual activity contribute to the mechanisms involved in the loss of spatial encoding at the early stages of AD.

Background

At present, Alzheimer’s disease (AD) is the most common form of dementia, and projections predict that this value could grow up three times in 2050 [1]. AD is a neurodegenerative disease characterized by the accumulation of beta-amyloid and phosphorylated tau in addition to synaptic and neuronal loss. At early stages, AD is expected to generate alterations in neural connectivity through the damage of neural circuits and the creation of aberrant networks, which are relevant for many cognitive skills [2].

The clinical diagnosis of AD is often reached when there is already considerable neuronal loss in large cerebral regions [3]. This selective neuronal loss contributes to memory loss and higher-order cognitive functions due to the disconnection of the neural circuits involved [4–7]. Loss of spatial memory has been

reported as one of the first signs in AD, showing the role of the neurodegenerative process in the hippocampus, a key part of the brain, in solving spatial navigation challenges [8–11]. The hippocampus and parietal, prefrontal, and occipital regions constitute the core network for navigation even in the prodromal and preclinical stages. However, an interesting association was the activation in young and elderly controls, but not in AD and MCI subjects, of several frontal lobe areas related to action planning sequences, including executive functioning, organization, error monitoring, and global response decision making [12–14]. A putative effective method of controlling disease progression is an early diagnosis and an appropriate management strategy that starts from the beginning of the cognitive decline. For this reason, one of the main challenges for developing treatment methods in all neurodegenerative diseases, especially AD, is to understand the pathological brain mechanisms underlying cognitive impairment [15, 16]. In this work we evaluate whether long-range Functional Connectivity (FC) alterations constitute part of the early mechanisms at the initial stages of Alzheimer's disease.

Methods

Participants

A total of thirty-eight individuals were recorded, 22 elderly cognitively healthy controls and 16 early AD (eAD), where the mean age was (70.32 (+/-7.79); 6 male) and (77.06 (+/-6.97); 8 male) years for the control and eAD group, respectively. The exclusion criteria for both groups were evidence of non-degenerative dementia (e.g., inflammatory, metabolic, or vascular etiology); dementia or mild cognitive impairment of doubtful origin; severe medical conditions that limited their ability to participate in the study (e.g., uncompensated diabetes, severe hypertension). The Scientific and Ethical Committee approved all procedures involving participants of the Clinical Hospital of the University of Chile Protocol number: 26/2015. In addition, all participants signed an informed consent previously approved by this Ethics Committee.

Neuropsychological testing

Cognitive functions were examined with the Clinical Dementia Rating scale (CDR) [17] and CDR Sum-of-Boxes (CDR-SOB) [18], a numeric scale used to quantify the severity of dementia (e.g., its stages). Also, the Montreal Cognitive Assessment (MoCA) [19], the Montreal Cognitive Assessment Memory Index Score (MoCA-MIS) [20], and the Minimental State Examination (MMSE) were used as a rapid screening instrument for mild cognitive dysfunction. A complete clinical evaluation, including full neuropsychological tests, was performed by a neurologist from the Department of Neurology of the Clinical Hospital of the Universidad de Chile, who was blind to the performance of the subjects in the navigation task. Participants were classified in cognitively unimpaired (CDR0) and early AD (eAD) based on their cognitive status.

The study involved 18 volunteers: 9 participants (eAD group) and 9 participants (control group) aged between 61–88 years. The eAD group consisted of patients with cognitive impairment with apparent memory deficits, with a global CDR 0.5, a CDR-SOB ≥ 1.5, and a MoCA-MIS ≤ 10, with two or fewer words

out of 5 of the MoCA tests recalled spontaneously. Also, eAD participants had a very mild loss of instrumental activities of daily living. Control participants were submitted to the same neurological and neuropsychological evaluations as the eAD group. The demographic data of the participants are shown in Table 1.

Table 1
Demographic characteristics and levels of cognitive function.

Characteristic	eAD number (%) or mean ± SD	Control Number (%) or mean ± SD	p value
Sample			
Size	9	9	
Age	76.67 ± 6.16	71.22 ± 8.48	0.2138
Range (min-max)	69–88	61–84	
Gender			0.6199
Male	2 (22.22%)	4 (44.44%)	
Female	7 (77.78%)	5 (55.56%)	
Education (years)	12.33 ± 4.03	16.89 ± 4.31	0.0299
Neuropsychological measures			
CDR-SOB scores	0.89 ± 0.22	0	< 0.001
MoCA scores	20.44 ± 3.32	29.22 ± 0.83	< 0.001
MoCA-MIS	9.56 ± 2.19	14.78 ± 0.44	< 0.001
MMSE scores	23.22 ± 2.05	29.78 ± 0.44	< 0.001

Continuous data are presented as mean (standard deviation), and categorical data are expressed as frequencies (%). Wilcoxon rank-sum test was used for age, education, CDR-SOB, MoCA, MoCA-MIS, and MMSE comparison between groups. The Chi-square test was applied for gender comparison (Fisher's exact test). Abbreviations: HC, Healthy controls; eAD, very early Alzheimer's Disease; CDR-SOB, Clinical Dementia Rating Scale Sum-of-Boxes; MoCA, Montreal Cognitive Assessment; MoCA-MIS, Montreal Cognitive Assessment Memory Index Score; and MMSE, Mini-mental State Examination.

Spatial navigation paradigms: Virtual Morris Water Navigation Task

Spatial exploration was assessed by the VMWM task in both eAD and control participants. The task was executed through an open-use program with support provided by its author [10]. The virtual environment

of the VMWM task simulates the traditional MWM, which consists of a circular pool located inside a room with visual cues on its four walls. The task is presented on a computer screen that the participant must navigate through the buttons of a keyboard to find a platform hidden under the water surface. The setup enables controlling a series of parameters to optimize the sensitivity of the task, related to characteristics of the visual cues and the location of the hidden platform, the maximum duration, and the number of trials. After finishing the task, the program stores in text files the information related to the route traveled, the latency to find the platform, and the relative percentages of the length of the path spent in each quadrant of the virtual pool.

All participants performed a well-established navigation task which was divided into three stages. Training (Stage I): this task involved finding the platform hidden under the water in a room furnished with visual clues on each of its walls. The platform became visible after one minute of exploration if the participant did not find it. Therefore, the participant needed to reach the platform to finish the trial. Before the end of the trial, the participant had 2 seconds to rotate in place to explore its position in the environment visually. This stage comprised four repetitions of the trial. The platform was kept in the same hidden position inside the pool, and the participant always started each repetition from a different position. Task I (Stage II): The participant had to find the platform hidden based on different visual cues to those presented in the training session as in the previous stage. The task included twenty trials divided into four groups. A two-minute break was considered among each group of trials. Similar to the training session, the platform was always kept in the same position inside the pool. The participant always started each repetition from a different position inside the pool. Task II (Stage III): in an equivalent room but including different visual cues, the participant had to select one of two visible platforms; only one represented the correct choice. A note on the screen indicated whether the platform chosen was correct. This task was used to control each participant's visual and psychomotor functioning, making it possible to rule out any deterioration in these parameters as plausible reasons for unsatisfactory performance in task I.

EEG recordings and eye-tracking

During the behavioral navigation task, the continuous acquisition of the electroencephalographic activity of each participant was carried out beneath adequate recording conditions. An EEG system of 32 + 8 channels was employed (8 external channels to measure electro-ocular activity and referential mastoid recording; BioSemi®). The acquired analog signal was filtered between 0 (real DC) and 1000 Hz before its conversion, sampled at 2048 Hz, and digitally converted with a precision of 24 bits. The recording system used a specific reference system (CRS-DRL) that allows unlimited data storage. After electrodes were located, the participant was installed in a suitable chair in front of the monitor where the VMWM task was displayed. The head was positioned on chin support to minimize movement during the task and allow optimal detection and recording of eye movements. Eye-tracking was performed using an Eyelink® 1000 system, which digitizes and stores eye-tracking data in a binary file convertible to text. The bi-dimensional position of the pupils was obtained at a frequency of 500 Hz. The system also automatically registers the occurrence of blinks, fixations, and ocular saccades based on user-defined initial setting parameters.

Data Analysis

Henceforth, all data analyses made in this study, including behavioral parameters of space navigation in the VMWM task, electroencephalographic signals, and eye-tracking data, were performed with MATLAB® (The MathWorks, Inc.). First, for behavioral data, the text files generated by the program after finishing the task were imported and analyzed using custom algorithms designed for these purposes, employing general functions of the basic software package. Second, the binary .bdf files generated were directly preprocessed using the Fieldtrip open-source toolbox for EEG signals. The eye-tracking binary data were initially converted to ASCII text files using the Eyelink® executable EDF2ASC.exe. Finally, the EYE-EEG MATLAB toolbox was used as a plugin of the EEGLAB package to import, visualize and verify the detected eye-tracking events and synchronize with the EEG signals [21].

EEG signals were visually inspected by a qualified clinical neurophysiologist to judge the collected signals' quality and reject abnormal recordings (i.e., epileptiform activity and abnormal basal rhythms). Then the segments of data presenting non-extractable artifacts were manually marked for the exclusion of the analysis. Offline filter settings were bandpass filter at 1–40 Hz (Butterworth, FIR). Next, artifact elimination was applied using ICA decomposition (fieldtrip toolbox) over the whole continuous record. Finally, noise components were identified in a semi-automated way, utilizing algorithms executed in the EYE-EEG package to detect ocular movement-related components.

Continuous EEG signals were segmented using the ocular tracking signal synchronized with the filtered EEG signal, between − 1000 and 3000 ms around the ocular fixations. To ensure that the data did not significantly bias, we evaluated the first 30 seconds of the records because the time of each participant was unsteady over the trials. Fixation-related epochs were consequently subjected to analyses in the time and frequency domains. First, the time-frequency decomposition was computed on the EEG epochs tapered by a sliding Hanning window, using the same fixed window length seconds for all frequency ranges of 1 and 40 Hz in steps of 1 Hz implemented at the time between − 750 and 1500 ms in steps of 10 ms. Second, we implement an analysis method multitaper based on multiplication in the frequency domain, obtaining finally output power-spectra (fieldtrip toolbox). First, for each time, frequency, and electrode, was calculated as the modulus of the mean across trials. Then, for each frequency, values of power-spectra were transformed to Z scores, normalizing by the corresponding mean and standard deviation of prestimulus time between − 750 and − 450 ms. Finally, these normalized values were compared for each time, frequency, and electrode between experimental groups.

We computed the coherence in two ways: first, performing time-frequency analysis on any time series trial data using the multitaper method, based on conventional tapers like Hanning to obtain the power and the cross-spectra, and in a second way using a method that performs frequency analysis on any time series trial data using a conventional single taper (e.g., Hanning) to obtain the complex Fourier-spectra (fieldtrip toolbox). The estimated coherence ranges from 0 to 1, whereby 0 means that the corresponding frequency components of both signals are linearly independent, and 1 means that the frequency components of the two signals give the maximum linear correlation. Thus, coherence estimation is a

valuable tool to observe and quantify the synchrony property of two EEG series, mainly when they are limited to some particular frequency bands [5, 6]. Coherences for delta (2–4 Hz), theta (4–7 Hz), alpha (7–13 Hz), beta (13–30 Hz), and gamma bands (30–40 Hz) were calculated as the mean coherence values of the epochs between 0 and 300 ms. To estimate whether the changes were primarily related to the impairment of short or long-range, coherences were calculated using the following electrodes: (O1, O2, PO3, PO4, CP1, CP2, C3, C4, F3, F4, F7, F8, Fp1, Fp2) that were frequently reported to be affected in AD progression. The EEG coherence calculation for each electrode pair generates a 14 x 14 (EEG channels selected) matrix showing the connectivity between all possible functionally independent brain areas in each frequency band. To examine the regional difference in coherence values, we subdivided the EEG channels into the following four groups: frontal (Fp1, Fp2, F3, F4, and FZ), parietal (FZ, C3, C4, CZ, and PZ), occipital (O1, O2, P3, P4, and PZ), and temporal (F7, F8, P7, and P8). Finally, we measured the effect sizes (Cohen's d) and an independent-sample t-test between groups considering the Beta coherence spectrum.

Eye-tracking analysis

Fixations and saccades were automatically identified based on the velocity (30°/s) and acceleration threshold (8000°/s2). Saccades longer than 5 ms and smaller than 100 ms and fixations between 50 and 800 ms were picked for further processing. In addition, blinks were defined as the absence of pupil data.

Statistics

Demographics and neuropsychological performance were divided into continuous variables expressed as mean and standard deviation (SD), while the categorical variables were expressed as frequencies (%). Wilcoxon rank-sum test was used for age, education, CDR-SOB, MoCA, MoCA-MIS, and MMSE comparison between groups. A chi-square test was used for gender comparison (Fisher's exact test). Differences in ocular behavior as the frequency of ocular movements (fixations and saccades) were measured using a nonparametric Wilcoxon rank-sum test between the control and eAD group. Additionally, we obtained a heat map of the probability of differences and a map of significant differences between the exploration performed by both groups. Finally, we conducted a rank-sum test as a statistical approach pixel by pixel on the image, performed at the 0.05 significance level.

Statistical tests based on permutations were applied to evaluate the differences between groups of the oscillatory activity, such as the time-frequency power spectral decomposition and coherence. The Montecarlo method was considered an estimator of the permutation's significance probabilities and critical values (two-tailed, alpha: $p < 0.01$, cluster correction, cluster-alpha: $p < 0.05$). Given many corrections applied to the number of electrodes to be compared between groups, we used cluster as a correction method that solves the Multiple Comparison Problem (MCP) [22, 23]. Moreover, we calculated effect sizes (Cohen's d) as the difference of the means of groups (control and eAD) divided by the weighted pooled standard deviations of the groups. Cohen's d effect size of 0.2 to 0.3 could be a "small" effect, around 0.5 a "medium" effect, and 0.8 to infinity, a "big" effect (a Cohen's d greater than 1 as possible). We estimated significant differences intragroup for the baseline in a beta-band coherence

region of interest (15–20 Hz and between 0–300 ms) using a statistical threshold criterion of effect size (> 0.5) and one-sample t-test (< 0.05). This threshold was applied to a chi-square test for intragroup ratios. The data were treated by MATLAB toolbox and Fieldtrip toolbox.

Results

The detailed demographic and neuropsychological assessment information is presented in Table 1. Nine patients diagnosed with eAD, and nine matched control participants were recruited for this study. We found no significant differences in the age distributions between the eAD (76,7 ± 6,2 years old) and the control groups (71,2 ± 8,5) years old); Wilcoxon Rank sum test, (p = 0.2138). Sex subgroups were the same in both groups (2 males [22.22%] and four males [44.44%] in the eAD and control groups, respectively; Fisher's exact test, (p = 0.6199). Years of education were 12,3 ± 4,0 years in eAD and 16,9 ± 4,3 in the control group (Wilcoxon Rank sum test, p = 0.0299). The MoCA score of the eAD group was 20.44 ± 3.32 (mean ± SE), and the MoCA-MIS score was 9.56 ± 2.19 (mean ± SE). The MoCA and MoCA-MIS scores of the control group were 29.22 ± 0.83 and 14.78 ± 0.44. There were no differences in the prevalence of diabetes, hypertension, or tobacco use between the eAD and the control groups.

Ocular behavior and visual exploring strategies

We first obtained a graphical representation of the visual eye fixations distributions per group, represented through heat maps. Then, a Gaussian filter was applied for each heat map seeking to normalize the location and duration of the eye fixations. The eye fixations in the control group were more focused in the central region (Fig. 1A). While the eAD group, the visual exploration was much more homogeneous in the image and without a clear preference on the Region of Interest that could guide the task's solution (Fig. 1B). We decided to calculate the absolute differences between groups with this approach as an example of visual exploration. Although both groups visually explored the center of the image in contrast to the periphery, we found the main differences in the intermediate image region. By comparing the absolute value of difference for both the control and the group with eAD, we observed that the control group had a high preference to fix the central area very close to a position on the water in the pool (the region where the platform could be located). In contrast, the eAD group focused on the upper midline without a defined focus in the target platform.

Additionally, we performed a comparison pixel-by-pixel of the visual exploration of the groups. We used level curves for the heat maps of the eye fixation with the normalized values. Furthermore, we applied a rank-sum test for all pixels of the heat map to obtain a probability of differences in the exploration with a color scale between 0 and 1, where the values closer to 1 (red color) were more likely to be different. This result highlights the lower central region, which could correspond to an area close to the hidden platform. The segment with statistical differences shown in red (Wilcoxon rank-sum test, p < 0.05). (Fig. 1C and 1D). To confirm that the visual exploration behavior of participants with eAD differed from that of controls and that their fixation targets were located more in the lateral, top, or bottom positions of the middle line, whereas controls fixated more on the straight-ahead position, we analyzed the distribution.

Eye fixation frequency distribution revealed a significant difference between control and eAD groups (KS test; D = 0.11, p = 0.0014). The participants with eAD had more eye fixations over the middle line and less bottom relative to controls (Fig. 2). These results confirm that both groups differ behaviorally in their visual exploration, reflecting their ability to process visual information.

Time-frequency analysis

Power spectra were performed to identify differences in a particular frequency band and use this range for subsequent functional connectivity analysis. We applied multiple time-frequency transformation (TF) windows in the frequency domain. The TF decomposition was achieved by generating epochs in the signal associated with the eye fixation and taking a baseline that considered − 750 to -450 ms before the event. Two examples of TF maps are shown for each group (Fig. 3). Moreover, we calculated the average per group for the Oz channel, where both the Control group and the eAD group showed a marked predominance of activity in the low-frequency spectrum, in particular, theta and alpha bands, but also an activity relevant in the beta band that went only recognized in the control group (Fig. 4A and 4B).

A two-tailed non-parametric cluster-based permutation test with an alpha error level of 0.01 for the Oz channel was performed to test for differences in the power between the groups. This test was conducted on the TF data from − 250 ms to 600 ms, which means that we include what happens eventually with the previous saccade, and after the origin of the fixation (adequate window to involve the visual event and its early cognitive processing) and this for a frequency range that considers low frequencies 2 Hz to 25 Hz. A Monte Carlo estimate of the permutation p-value was computed by randomly permuting condition labels (N = 1000). We observed significant differences in the beta band between 15Hz to 18 Hz for the first 250 ms post-fixation and the same effect between 17 Hz to 20 Hz for the 250 to 600 ms post-fixation (Fig. 4C). Additionally, the power difference (control - eAD) is shown in a topographic map for the beta frequency band, within the range of 15 Hz to 20 Hz in the time interval between 0 and 200 ms (Fig. 4D).

Functional connectivity analysis

Coherence can be considered a measure of normalized linear synchrony of different EEG series in the frequency domain or a functional substrate of activity patterns with high relative power, such as an ERP. Here, coherence analysis was applied to pairwise EEG channel subgroups for the eAD and control groups in the beta frequency band. The analysis of the frequency spectrum to Cluster-based permutation tests mentioned above had significant group differences. In particular, the activity of this component was associated with visual processing at the time when we expect to get connectivity differences between both groups concerning the visual information processing.

The mean coherence between 14 channels of eAD and the control group in the beta frequency band (15 Hz to 20 Hz) is shown in (Figs. 5A and 5B). The mean coherence distributions of the two groups were symmetrical, indicating the presence of fast bidirectional transmission of information between brain areas. These pairwise electrodes were principally related to the frontoparietal activity, whose functions are widely associated with working memory and, in particular, relevant in visual working memory and visual attention. The diagonal of the coherence matrix was all = 1 because the EEG signal could achieve

complete synchrony with itself. The coherence matrices of the two groups were complex and initially very similar. Then, however, we calculated the connectivity matrices with baseline correction from − 750 to -450 ms. In the control group (Fig. 5C), there were more areas of high (red color) values of coherence than that of the eAD group (Fig. 5D). While in the eAD group, the low values of coherence were distributed in areas like frontal and frontoparietal areas for the beta band. The matrix of P values returned by a one-sample t-test between groups (Fig. 5E) showed the significant difference uncorrected on coherence.

To know the impact of these results, the effect size of the coherence spectrum was estimated. The values considered the Frontoparietal-occipital axis, where the biggest differences between groups were appreciated. The effect size was obtained by using Cohen's d. This value was calculated by subtracting the mean from the eAD group minus the mean of the Control group and dividing by the standard deviation of the population to which both groups belong. These values could be interpreted as small (Cohen's d = 0.2 to 0.3), medium (Cohen's d = 0.5 to 0.7) and large (Cohen's d > 0.8) values. We proposed to consider the medium and large values in the matrix (Fig. 5F).

Additionally, only the large values of Cohen's d were used in a topographic map highlighting which areas could impact the participants' behavioral performance (Fig. 6A). This map of the effect size showed the regions that varied the most between groups and could account for the early behavioral differences of the eAD participants for the strategies used in the virtual navigation task. We found the more prominent changes in coherence were essentially frontoparietal and suggest that lower activation or synchronization in prefrontal cortices may be the cause of worse spatial navigation.

Then, we created a binary connectivity matrix. Here, the threshold is set as a combination of values calculated previously in the beta frequency band (15 Hz to 20 Hz). Firstly, we considered an effect size (> 0.5); secondly, when the P-value matrix for one-sample t-test is (< 0.05). The color scale represents in black significant coherence differences from the baseline time (-750 to -450 ms). At the same time, the white color depicts no differences from baseline time for the activity of the pairwise comparison. The statistical analysis results of the intragroup coherence for the control connectivity matrix show many pairwise comparisons with significant differences (Fig. 6B). The eAD matrix shows only one electrode pair with significant brain activity changes (Fig. 6C). Finally, we show the topographic distribution of electrode pairs with significant coherence differences from baseline time by groups, using as a threshold the $p < 0.05$ and Cohen's $d > 0.5$ (Fig. 6D). Based on these results, we suggest that the long and short-distance synchrony and Intra and Interhemispheric connections that present a higher degree of differences to the coherence belong to the frontoparietal region of the brain. This could be the consequence of less effective planning of navigation routes since this region is critical for executive functions, including planning, organization, error monitoring, and decision making.

Discussion

Despite the vast progress of recent years in the study of AD, the principal mechanisms involved in cognitive deficits in the disease are still unclear. This study compared ocular behavior and the functional

connectivity in control vs. eAD subjects in a sensitive early detection test of cognitive impairment [24–28]. Our results showed a significant difference in visual exploration between the groups; however, the fixing area percentage did not show significant differences. Additionally, early differences were observed in the beta band activity (15 Hz to 20 Hz) that has been related to the execution of cognitive processes. Finally, the coherence between different cortical regions, significant effect differences were observed between groups in the prefrontal region in the beta band with consequences for less effective planning of navigation strategies.

Very early Alzheimer's disease and ocular behavior impairments

Patients with a diagnosis of eAD performed significantly different exploration strategies than the control group to reach the visual keys in the task. These findings reaffirm the notion observed in other studies that identified increased instability in fixation, enhanced latency of voluntary exits, the direction of microsaccades, greater anti-saccadic errors, and decreased correction of this anti-saccadic error in AD participants [29–30]. The strategies of visual exploration based on the distribution of the fixations were analyzed employing heat maps. They were described as an early manifestation of AD alterations of executive functions and different visual parameters such as visuospatial skills, processing, and selective visual attention [31]. We showed that the fixations in the control group were preferably concentrated on the objects being relevant for the task (visual keys and possible platform location), unlike the eAD group, where the visual exploration was more homogeneous in the image and without a clear preference on regions of interest that could guide to solve the task. Furthermore, the participants with eAD had more eye fixations over the middle line and less bottom relative to controls. These results could suggest that visual exploration strategies of the eAD participants can be associated with attention deficiencies and the involvement of prefrontal networks and visual attention WM [32].

Early electrophysiological changes and role of prefrontal Beta band coherence in eAD.

Our electrophysiological results showed differences in the application of the spatial navigation task between the groups. The spectral power analysis through the time-frequency maps, presenting differences in activity in the theta frequency ranges, alpha, and significantly in the beta band (15 Hz to 20 Hz), confirmed by the analysis of Cluster-based permutations tests. These findings are consistent with a large number of studies that reported increases in the theta band and a decrease in the alpha and beta band of patients with AD [33]. Other studies even attributed the reduction in the alpha band and reduced beta power in the parietal and occipital regions as a differentiating factor between normal aging, MCI, and AD [34–41]. Particularly, the beta band has been related to memory processes, and their decrease in the eAD group could be associated with difficulties in spatial navigation when the reactivation of memories is necessary to find the platform by visual cues [42].

Beta oscillations have been described in many studies of perceptual, cognitive, and motor processes. Although a single term could not entirely explain its function, the more accepted descriptions ascribed a role of the beta band in interneural communication of inhibitory networks and high executive demands [43, 44], while synchronization might be involved in sensory processing [45]. Our results showed a reduction in the beta band functional connectivity in the eAD group in prefrontal cortices. Both alpha and beta frequencies are associated with many functions that represent top-down influences. Still, particularly beta oscillations are crucial to long-distance communication between cortical regions, with the function of maintaining a constant update of brain status [42].

Additionally, the prefrontal cortex could be involved in associative learning in navigation and changing strategies and engaged in processes to search for specific objectives such as selecting the best route or trajectories in space navigation processes [46]. Our results, as well as previous studies, showed that selective visual attention is sensitive in eAD. Besides, disconnections between brain regions were described to play an essential role in cognitive impairment in AD, with reduced synchrony as a marker [16, 47–49].

Some studies have proposed that activating the right prefrontal cortex (PFC) during spatial WM tasks was described in young adults. In contrast, older adults presented bilateral activation of PFC as a compensatory response to cognitive impairment. Likewise, during particular memory tasks (such as coding complex visual scenes), healthy older adults also showed bilateral hyperactivation of the frontal cortex. Furthermore, during the MCI to AD progression, it has been proposed that a disintegration of the compensatory networks occurs due to the observed lack of activity of the lateral regions of the PFC, the precuneus, and posterior parietal cortex. These regions are all involved in the executive function compared to controls[50,51]. These findings are consistent with our proposed that the symptoms observed in patients with eAD are closely related to a loss of functional connectivity, reflected by physiological changes and an attenuation of the electrical activity [48, 49, 52, 53].

As we supposed, spatial navigation impairments can be associated with early mechanisms of cognitive deterioration in the progression to AD. This task joints the occipital, parietal, and frontal cortices functions. We already know that the navigation abilities depend on the occipital cortices for the early processing of visual information and the parietal and hippocampal cortices on the generation of the cognitive map and egocentric/allocentric navigation strategies. At the same time, the frontal cortex is relevant for its participation in the decision, development, and planning of actions [12]. A study by Coughlan showed that morphological changes (in particular the accumulation of Aβ in the cerebral cortex) follow a typical course of progression, which coincides with the structures involved in spatial navigation. Therefore, it seems that these structural changes are not isolated and that the functional alterations are later.

Furthermore, these changes occur in regions that appear to be involved in the networks necessary to establish functional connectivity in navigation tasks [13]. In brief, it is essential to understand the proposed mechanism of coordinate participation of all these mentioned cortices for better performance.

We suggest an operational model whose functionality depends on many structures, where each area's integrity matters but the generated functional connectivity. Thus, the spatial navigation impairments are consistent with the progress of the loss of cognitive skills and less functional connectivity in very early AD [8–11, 15, 16].

Limitations

Our work provides new evidence for a dysfunctional neural pattern in visuospatial processing, higher order attention and executive function in early AD patients, but also reveals some limitations that should be mentioned. First, this study is limited by the statistical approach as it is necessary to apply many corrections for the number of electrodes that were compared between the study groups. To solve the problem of multiple comparisons (MCP), the cluster-based permutation test was used as a correction method in the time-frequency analysis and in the data coherence analysis [22, 23]. In addition, the timing of trials was variable within subjects and between groups. However, this random temporal variability was corrected using the first 30 seconds of the recordings, as each participant's timing was unstable across trials, avoiding systematic bias.

Conclusions

This study showed early electrophysiological alterations in the eAD group in the prefrontal cortex. These changes could play a critical role in executive functions, planning, organization, error monitoring, and decision-making for spatial navigation and predictive motor planning [11, 14, 54]. Thus, we can conclude that the study of long-range functional connectivity in early stages could help predict AD progression. Finally, this study contributes to a better understanding of the mechanisms underlying cognitive impairment in AD and opens the door to better therapeutic management by identifying critical periods of change. This could provide the possibility of intervening in the system with the generation of more effective therapies when changes are still reversible and not when neurodegenerative processes have already been installed.

Declarations

Acknowledgements

First, we would like to acknowledge the efforts of our research participants. We would also to thank Cecilia Babul and Cristian Lopez for their technical assistance.

Authors ‘contributions

Conceptualization (IPR, APL, PEM), methodology (IPR, EB, APM, PEM), formal analysis (IPR, RMS, SM), investigation (IPR, RMS, SM, EB, MIB, APL, PEM), data curation (IPR, RMS, SM), writing—original draft (IPR), writing—review and editing (IPR, RMS, SM, EB, MIB, APL, PEM), visualization (IPR), supervision

(PEM), and funding acquisition (IPR, APL, PEM). The authors read and approved the final version of the manuscript.

Funding

This research was supported by CONICYT grants FONDECYT 1150736, FONDECYT 1190318, ICM P-09-015 and CONICYT-PFCHA/Doctorado Nacional/2018 – 21180413, and with the support of The Puelma Foundation.

Availability of data and materials

The datasets used and/or analyzed during the current study are available from the corresponding author on reasonable request.

Ethics approval and consent to participate

The Scientific and Ethical Committee reviewed and approved all procedures involving participants of the Clinical Hospital of the University of Chile Protocol number: 26/2015. All protocols conform to the principles of the Declaration of Helsinki. In addition, all participants signed an informed consent previously approved by this Ethics Committee.

Consent for publication

Not applicable.

Competing interests

The authors declare that they have no competing interests.

References

1. Reitz C, Brayne C, Mayeux R. Epidemiology of Alzheimer disease. Nat Rev Neurol; 2011;7:137–152.
2. Sarter M, Bruno JP. Developmental origins of the age-related decline in cortical cholinergic function and associated cognitive abilities. Neurobiol Aging. 2004;25:1127–1139.
3. Hampel H, Wilcock G, Andrieu S, et al. Biomarkers for Alzheimer's disease therapeutic trials. Prog Neurobiol. 2011;95:579–593.
4. Delacourte A, David JP, Sergeant N, Buée L, Wattez A, Vermersch P, Ghozali F, Fallet-Bianco C, Pasquier F, Lebert F, Petit H DMC. The biochemical pathway of neurofibrillary degeneration in aging and Alzheimer's disease. Neurology. 1999;52:1158–1165.
5. Dauwels J, Vialatte F, Musha T, Cichocki A. A comparative study of synchrony measures for the early diagnosis of Alzheimer's disease based on EEG. Neuroimage; 2010;49:668–693.
6. Dauwels J, Vialatte F, Cichocki A. Diagnosis of Alzheimer's Disease from EEG Signals: Where Are We Standing? Curr Alzheimer Res. 2010;999:1–19.

7. Dauwels J, Srinivasan K, Ramasubba Reddy M, et al. Slowing and loss of complexity in Alzheimer's EEG: Two sides of the same coin? Int J Alzheimers Dis. 2011;2011.
8. Pai MC, Jacobs WJ. Topographical disorientation in community-residing patients with Alzheimer's disease. Int J Geriatr Psychiatry. 2004;19:250–255.
9. Klimkowicz-Mrowiec A, Slowik A, Krzywoszanski L, Herzog-Krzywoszanska R, Szczudlik A. Severity of explicit memory impairment due to Alzheimer's disease improves effectiveness of implicit learning. J Neurol. 2008;255:502–509.
10. Hamilton DA, Johnson TE, Redhead ES, Verney SP. Control of rodent and human spatial navigation by room and apparatus cues. Behav Processes. 2009;81:154–169.
11. Etchamendy N, Konishi K, Pike GB, Marighetto A, Bohbot VD. Evidence for a virtual human analog of a rodent relational memory task: A study of aging and fMRI in young adults. Hippocampus. 2012;22:869–880.
12. Vann SD, Aggleton JP, Maguire EA. What does the retrosplenial cortex do? Nat Rev Neurosci. Nature Publishing Group; 2009;10:792–802.
13. Coughlan G, Laczó J, Hort J, Minihane AM, Hornberger M. Spatial navigation deficits — Overlooked cognitive marker for preclinical Alzheimer disease? Nat Rev Neurol. 2018;14:496–506.
14. Sneider JT, Cohen-Gilbert JE, Hamilton DA, et al. Adolescent Hippocampal and Prefrontal Brain Activation During Performance of the Virtual Morris Water Task. Front Hum Neurosci. 2018;12:1–14.
15. Alberdi A, Aztiria A, Basarab A. On the early diagnosis of Alzheimer's Disease from multimodal signals: A survey. Artif Intell Med. 2016;71:1–29.
16. Tait L, Stothart G, Coulthard E, Brown JT, Kazanina N, Goodfellow M. Network substrates of cognitive impairment in Alzheimer's Disease. Clin Neurophysiol. 2019;130:1581–1595.
17. Morris JC. The clinical dementia rating (cdr): Current version and scoring rules. Neurology. 1993;43:2412–2414.
18. O'Bryant SE, Waring SC, Cullum CM, et al. Staging dementia using clinical dementia rating scale sum of boxes scores: A Texas Alzheimer's research consortium study. Arch Neurol. 2008;65:1091–1095.
19. Nasreddine, Z. S., Phillips, N. A., Bédirian, V., Charbonneau, S., Whitehead, V., Collin, I., Cummings, J. L., Chertkow H. The Montreal Cognitive Assessment, MoCA: A Brief Screening Tool For Mild Cognitive Impairment. J Am Geriatr Soc. 2005;53:695–699.
20. Julayanont P, Brousseau M, Chertkow H, Phillips N, Nasreddine ZS. Montreal Cognitive Assessment Memory Index Score (MoCA-MIS) as a predictor of conversion from mild cognitive impairment to Alzheimer's disease. J Am Geriatr Soc. 2014;62:679–684.
21. Delorme A, Makeig S. EEGLAB: An open-source toolbox for analysis of single-trial EEG dynamics including independent component analysis. J Neurosci Methods. 2004;134:9–21.
22. Mike X Cohen. Analyzing neural time series data: theory and practice. 1st ed. The MIT Press; 2014.
23. Maris E, Schoffelen JM, Fries P. Nonparametric statistical testing of coherence differences. J Neurosci Methods. 2007;163:161–175.

24. Weniger G, Ruhleder M, Lange C, Wolf S, Irle E. Egocentric and allocentric memory as assessed by virtual reality in individuals with amnestic mild cognitive impairment. Neuropsychologia; 2011;49:518–527.
25. Laczó J, Andel R, Vlček K, et al. Spatial navigation and APOE in amnestic mild cognitive impairment. Neurodegener Dis. 2011;8:169–177.
26. Gazova I, Vlcek K, Laczó J, et al. Spatial navigation-A unique window into physiological and pathological aging. Front Aging Neurosci. 2012;4:1–6.
27. Gazova I, Laczó J, Rubinova E, et al. Spatial navigation in young versus older adults. Front Aging Neurosci. 2013;5:1–8.
28. Tarnanas I, Tsolaki A, Wiederhold M, Wiederhold B, Tsolaki M. Five-year biomarker progression variability for Alzheimer's disease dementia prediction: Can a complex instrumental activities of daily living marker fill in the gaps? Alzheimer's Dement Diagnosis; 2015;1:521–532.
29. Anderson TJ, MacAskill MR. Eye movements in patients with neurodegenerative disorders. Nat Rev Neurol; 2013;9:74–85.
30. Kapoula Z, Yang Q, Otero-Millan J, et al. Distinctive features of microsaccades in Alzheimer's disease and in mild cognitive impairment. Age (Omaha). 2014;36:535–543.
31. Chehrehnegar N, Nejati V, Shati M, et al. Early detection of cognitive disturbances in mild cognitive impairment: a systematic review of observational studies. Psychogeriatrics. 2020;20:212–228.
32. Belleville S, Bherer L, Lepage É, Chertkow H, Gauthier S. Task switching capacities in persons with Alzheimer's disease and mild cognitive impairment. Neuropsychologia. 2008;46:2225–2233.
33. Aghajani H, Zahedi E, Jalili M, Keikhosravi A, Vahdat BV. Diagnosis of early Alzheimer's disease based on EEG source localization and a standardized realistic head model. IEEE J Biomed Heal Informatics. 2013;17:1039–1045.
34. Coben LA, Danziger W, Storandt M. A longitudinal EEG study of mild senile dementia of Alzheimer type: changes at 1 year and at 2.5 years. Electroencephalogr Clin Neurophysiol. 1985;61:101–112.
35. Huang, C., Wahlund, L., Dierks, T., Julin, P., Winblad, B., Jelic V. Discrimination of Alzheimer's disease and mild cognitive impairment by equivalent EEG sources: a crosssectional and longitudinal study. Clin Neurophysiol. 2000;111:1961–1967.
36. Jeong J. EEG dynamics in patients with Alzheimer's disease. Clin Neurophysiol. 2004;115:1490–1505.
37. Kwak YT. Quantitative EEG Findings in Different Stages of Alzheimer's Disease Subjects and Clinical Scale. J Clin Neurophysiol •. 2006;23:457–462.
38. Rossini PM, Del Percio C, Pasqualetti P, et al. Conversion from mild cognitive impairment to Alzheimer's disease is predicted by sources and coherence of brain electroencephalography rhythms. Neuroscience. 2006;143:793–803.
39. Babiloni C, Frisoni GB, Vecchio F, et al. Stability of clinical condition in mild cognitive impairment is related to cortical sources of alpha rhythms: An electroencephalographic study. Hum Brain Mapp.

2011;32:1916–1931.

40. Ruiz-Gómez SJ, Gómez C, Poza J, et al. Measuring alterations of spontaneous EEG neural coupling in alzheimer's disease and mild cognitive impairment by means of cross-entropy metrics. Front Neuroinform. 2018;12:1–11.
41. Li R, Nguyen T, Potter T, Zhang Y. Dynamic cortical connectivity alterations associated with Alzheimer's disease: An EEG and fNIRS integration study. NeuroImage Clin; 2019;21:101622.
42. Guran CA, Herweg NA, Bunzeck N. Age-related decreases in the retrieval practice effect directly relate to changes in alpha-beta oscillations. J Neurosci. 2019;39:4344–4352.
43. Guevara MA, Cruz Paniagua EI, Hernández González M, et al. EEG activity during the spatial span task in young men: Differences between short-term and working memory. Brain Res; 2018;1683:86–94.
44. Hou F, Liu C, Yu Z, et al. Age-related alterations in electroencephalography connectivity and network topology during n-back working memory task. Front Hum Neurosci. 2018;12.
45. Singer W. Synchronization of cortical activity and its putative role in information processing and learning. Annu Rev Physiol. 1993;55:349–374.
46. Zhong JY, Moffat SD. Extrahippocampal contributions to age-related changes in spatial navigation ability. Front Hum Neurosci. 2018;12:1–8.
47. Delbeuck X, Collette F, Van der Linden M. Is Alzheimer's disease a disconnection syndrome?. Evidence from a crossmodal audio-visual illusory experiment. Neuropsychologia. 2007;45:3315–3323.
48. Wang R, Wang J, Yu H, Wei X, Yang C, Deng B. Decreased coherence and functional connectivity of electroencephalograph in Alzheimer's disease. Chaos. 2014;24:1–11.
49. Engels MMA, Hillebrand A, Van Der Flier WM, Stam CJ, Scheltens P, Van Straaten ECW. Slowing of hippocampal activity correlates with cognitive decline in early onset alzheimer's disease. An MEG study with virtual electrodes. Front Hum Neurosci. 2016;10:1–13.
50. Clément F, Gauthier S, Belleville S. Executive functions in mild cognitive impairment: Emergence and breakdown of neural plasticity. Cortex. 2013;49:1268–1279.
51. Kirova AM, Bays RB, Lagalwar S. Working Memory and Executive Function Decline across Normal Aging, Mild Cognitive Impairment, and Alzheimer's Disease. Biomed Res Int. 2015;2015.
52. Babiloni C, Visser PJ, Frisoni G, et al. Cortical sources of resting EEG rhythms in mild cognitive impairment and subjective memory complaint. Neurobiol Aging [online serial]. Elsevier Inc.; 2010;31:1787–1798.
53. Blinowska KJ, Rakowski F, Kaminski M, et al. Functional and effective brain connectivity for discrimination between Alzheimer's patients and healthy individuals: A study on resting state EEG rhythms. Clin Neurophysiol; 2017;128:667–680.
54. Morellini F. Spatial memory tasks in rodents: What do they model? Cell Tissue Res. 2013;354:273–286.

Figures

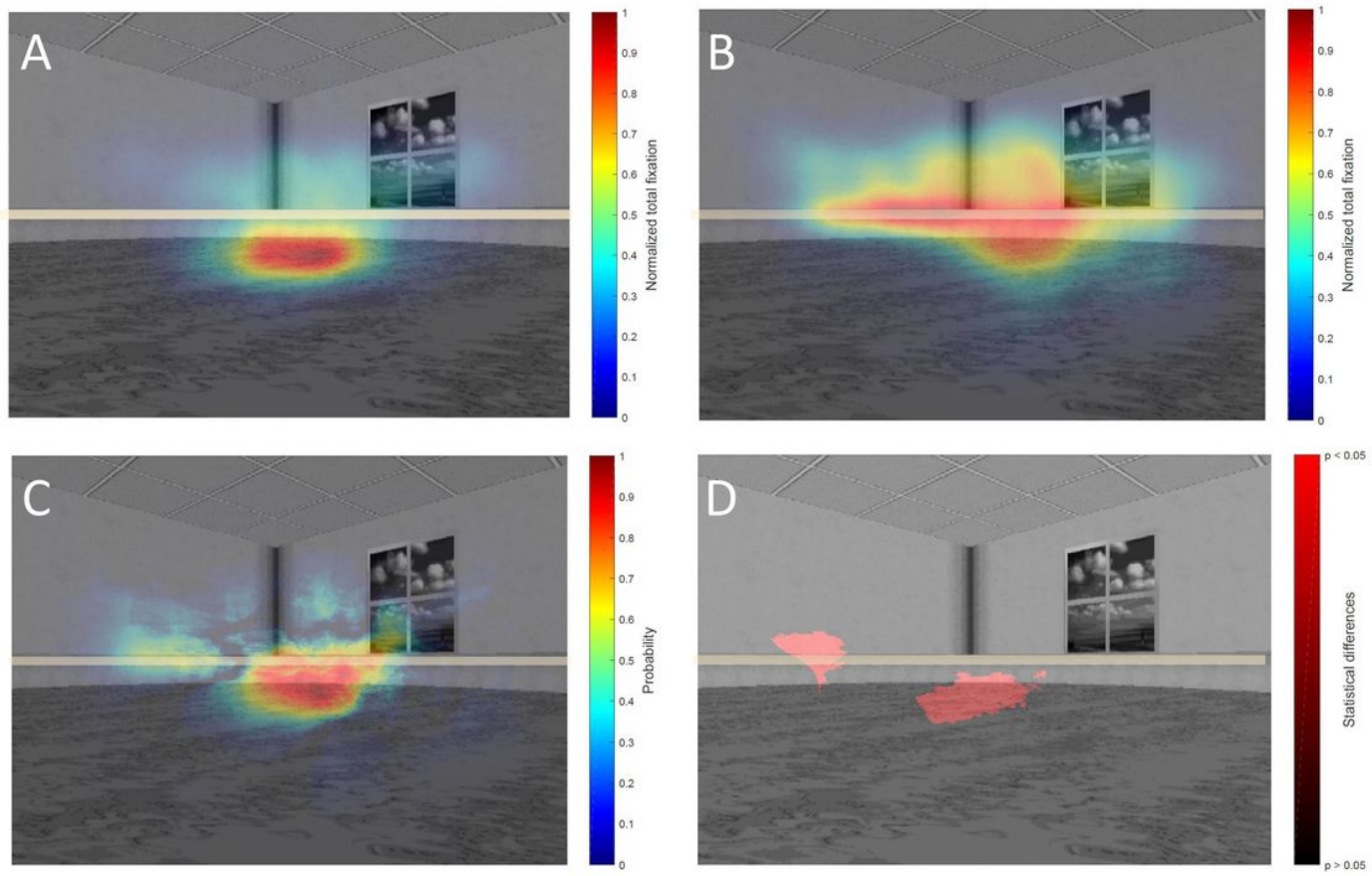

Figure 1

Figure 1

Heat map of the spatial distribution of eye-fixation in control and eAD groups. Heat map of visual fixations of the control group (a), showing high fixation density in the center/below the horizontal midline, and of the eAD group (b), demonstrating a less localized exploration. Warmer colors represent a higher number of fixations. c) Heat map of the probability differences in visual exploration. Again, warmer colors represent a higher probability. d) Regions with statistical differences in visual exploration between control and eAD group. The red path represents statistical differences (Wilcoxon rank-sum test, $p < 0.05$). The horizontal gray line represents the central region of the image.

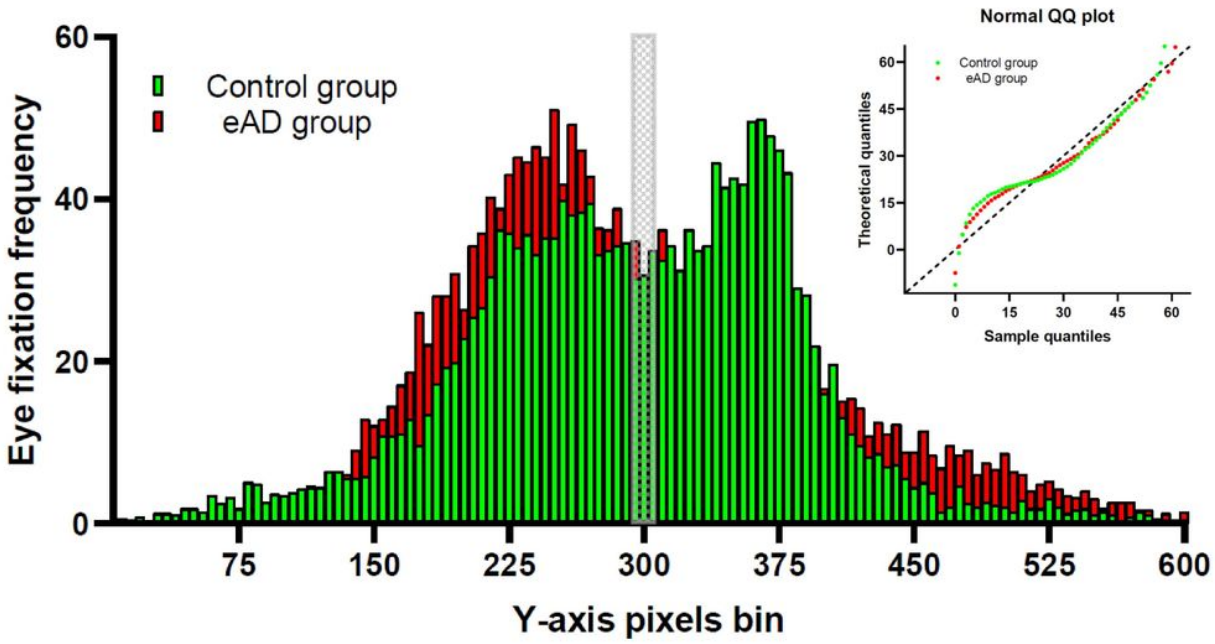

Figure 2

Figure 2

Eye-fixation frequency distribution of the Control and eAD groups. Comparison eye fixation frequency distribution in Y-axis pixels bin between Control and eAD groups. Kolmogorov-Smirnov test comparison cumulative fixation fraction (KS test; D = 0.11, p = 0.0014). Green: control group, red: eAD group. The gray block represents the central region of the image.

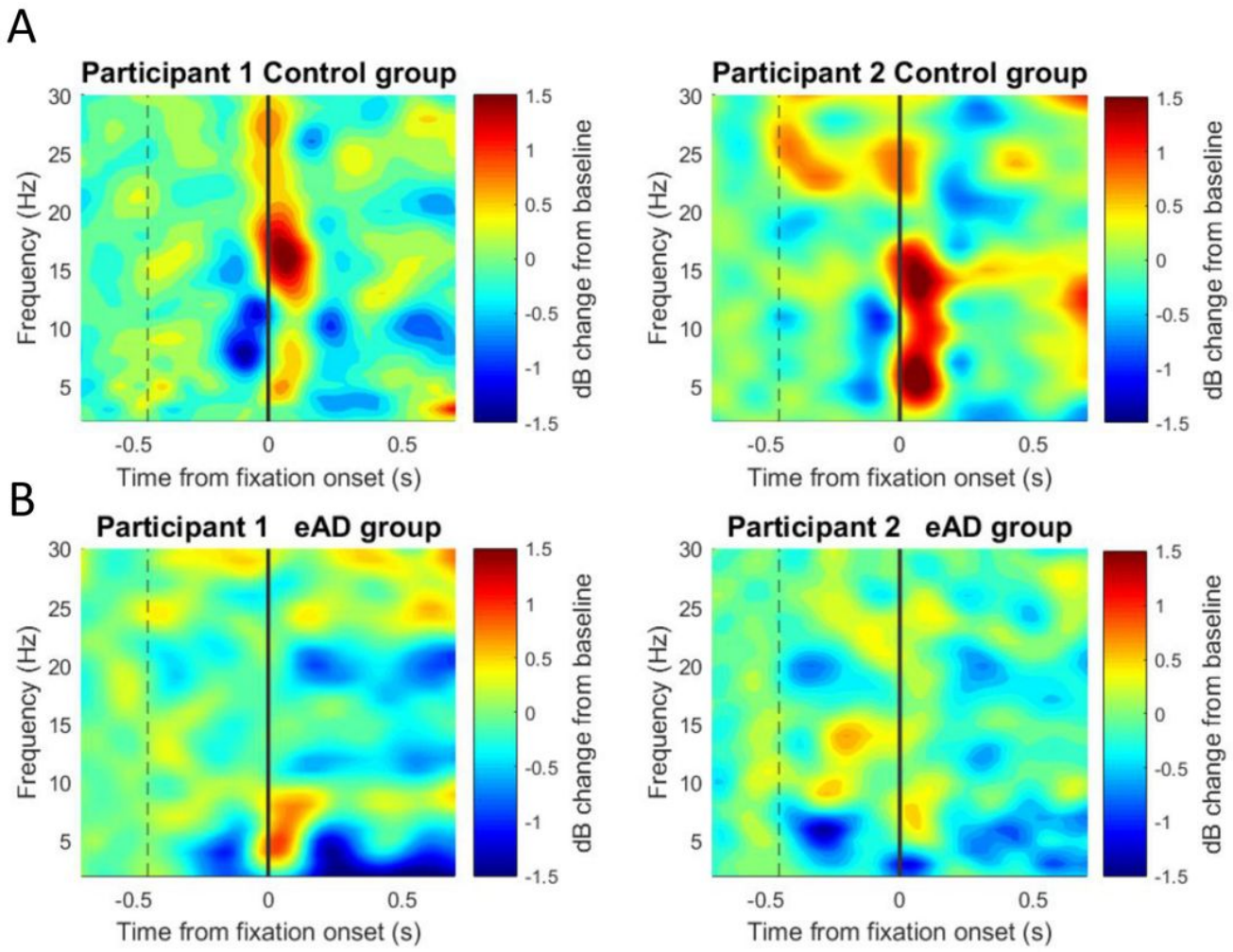

Figure 3

Figure 3

Power spectrogram of the EEG Oz channel. Time-frequency power spectral decomposition of the EEG data at the Oz electrode of two participants from the Control (a) and eAD groups. The solid vertical line represents the zero time at the beginning of eye fixation, and the dashed line indicates the start of the baseline recording. The color scale represents the percentage of change relative to the baseline period of -750 to -450 ms and normalized in decibels.

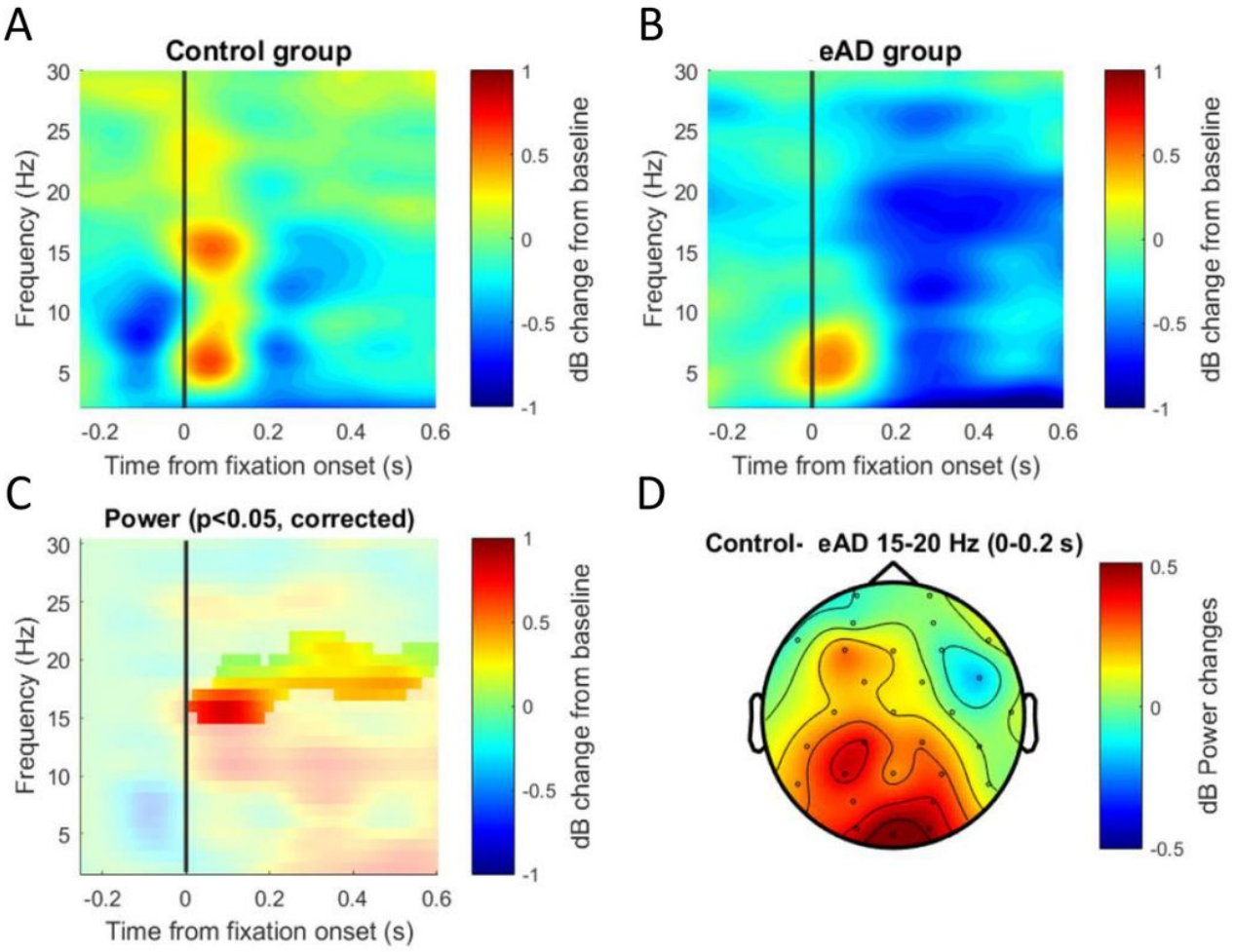

Figure 4

Figure 4

Time-frequency maps of the EEG Oz channel. Time-frequency power spectral decomposition of the EEG data of the Control (a) and eAD (b) groups. c) Cluster-based permutation test on time-frequency activity of the Oz channel. The analysis considered 1000 permutations to determine the cut-off alpha = 0.025 to two tails, resulting in significant differences in the beta band between 15-20 Hz. d) Topographical map from the averaged differences in power data. The solid line (vertical line) represents the zero time at the beginning of eye fixation. The color scale represents the percentage of change relative to the baseline period of -750 to -450 ms and normalized in decibels.

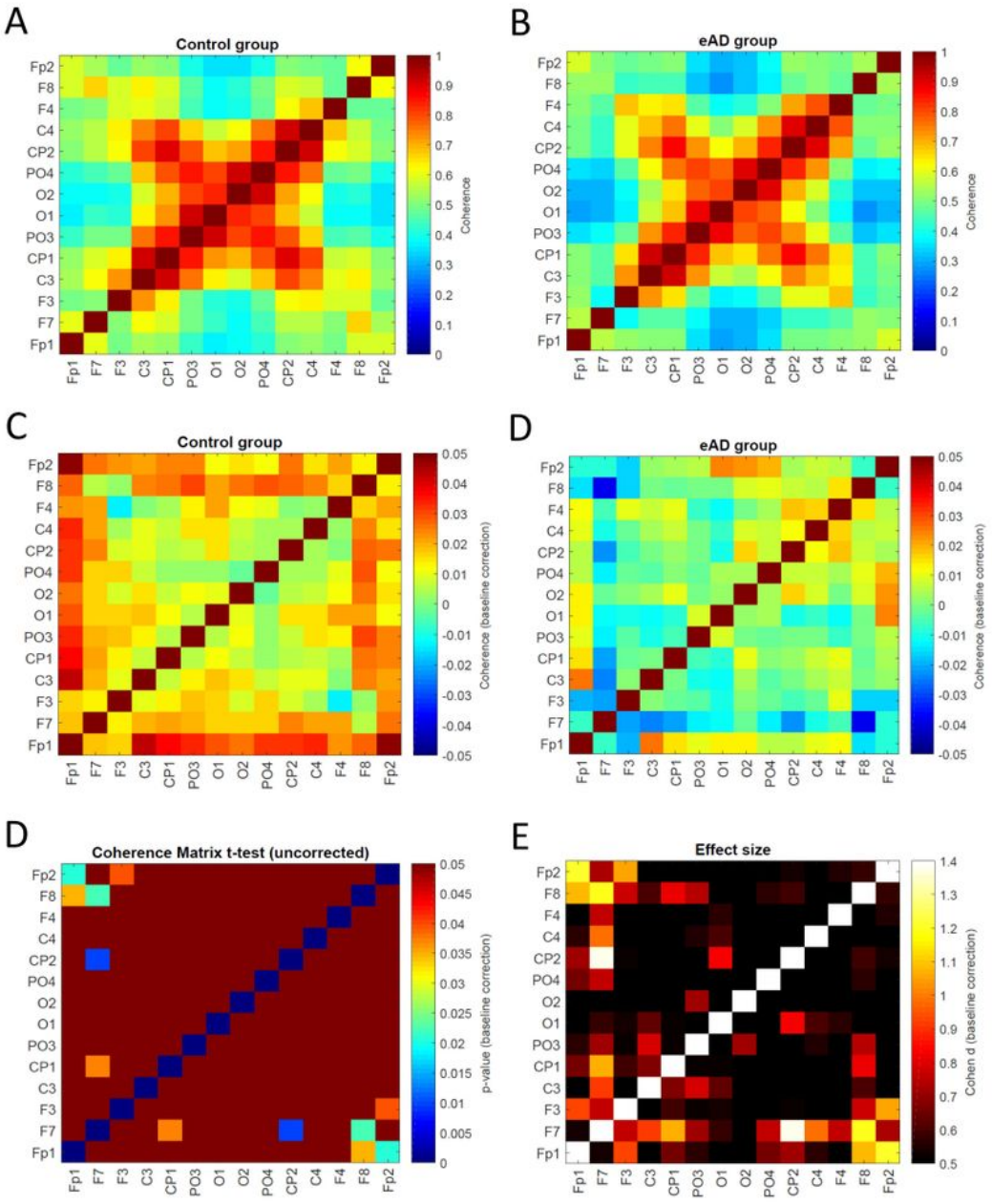

Figure 5

Figure 5

Coherence Beta (15-20 Hz) connectivity matrices from 0 to 300 ms. Absolute Coherence matrix for the Control a) and the eAD b) groups. Connectivity matrices with baseline correction from -750 to -450 ms c) Coherence matrix for the control group, d) Coherence matrix for the eAD group. The color scale represents low (blue) and high (red) coherence between each pair of electrodes. e) Matrix of P-value of the two groups obtained by t-test, the highest value with red color, and f) Matrix of differences between groups for

an effect size > 0.5 Cohen's d statistic (medium-large effect size). Thus, the color scale represents in black (dark color) medium differences of effect size and in white (light color) marked differences of effect size for the pair of electrodes.

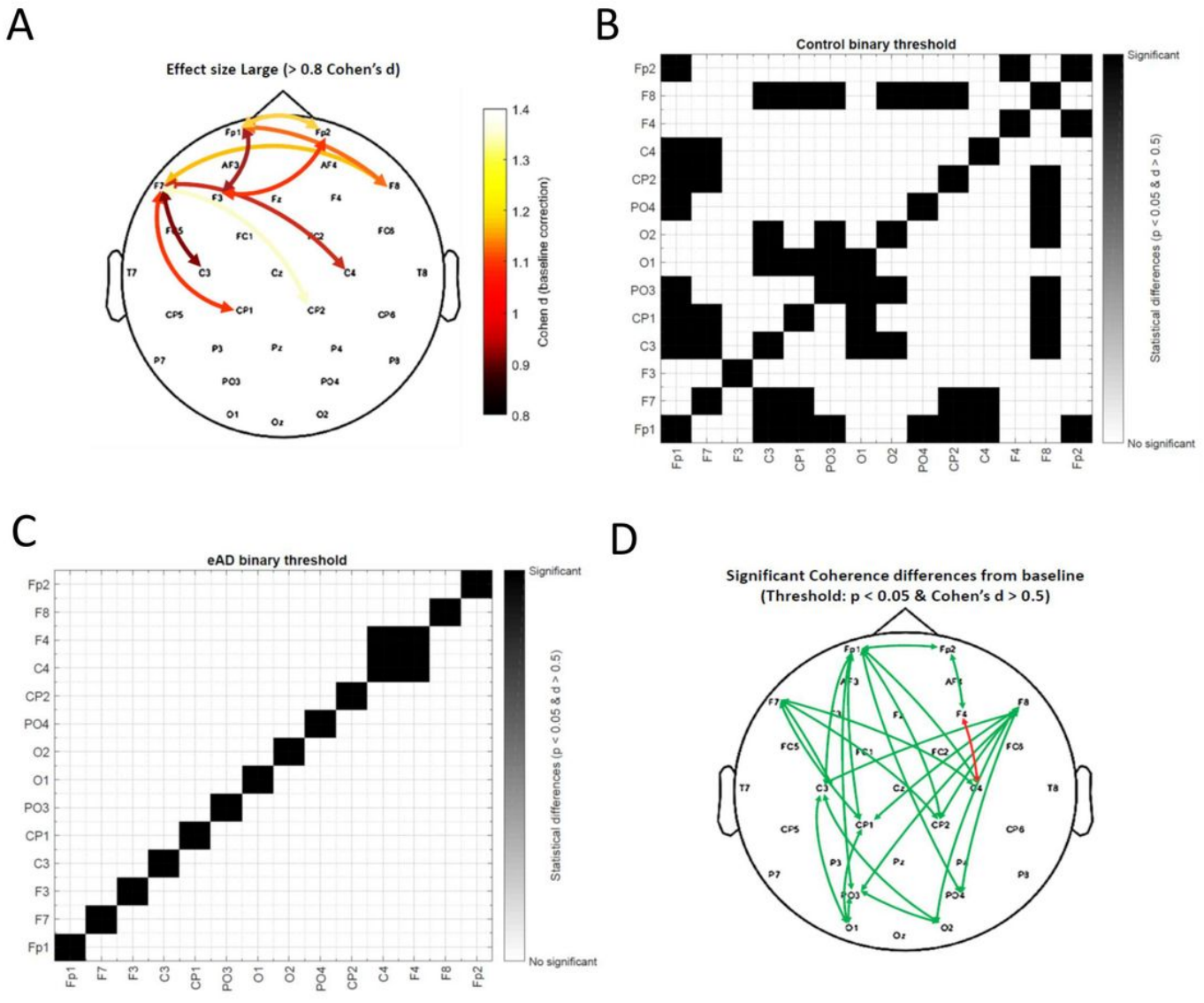

Figure 6

Figure 6

Effect size topographic map and Threshold value Matrix. a) Topographic distribution of electrode pairs with large value effect size (> 0.8 Cohen's d statistic). The color scale represents in white (light color) a marked difference effect size for the pair of electrodes. Matrix of Control (b), and eAD (c) groups. The color scale represents in black significant coherence differences for the baseline period (-750 to -450 ms). In white, there is no difference for baseline period for the activity of the electrode pair, using as a

threshold the $p < 0.05$ & Cohen's d statistic > 0.5. d) Topographic distribution of electrode pairs with significant coherence differences from baseline period by groups. The green arrow represents the control group and the red arrow the eAD group.